Available online at www.sciencedirect.com
SCIENCE DIRECT
Journal of Magnetic Resonance 180 (2006) 229–235
JMR Journal of Magnetic Resonance
www.elsevier.com/locate/jmr

Self-diffusion measurements by a mobile single-sided NMR sensor with improved magnetic field gradient

D.G. Rata, F. Casanova, J. Perlo, D.E. Demco, B. Blümich *

Institut für Technische Chemie und Makromolekulare Chemie, Rheinisch-Westfälische Technische Hochschule, Worringerweg 1, D-52056 Aachen, Germany

Received 7 January 2006; revised 24 February 2006
Available online 20 March 2006

Abstract

A simple and fast method of measuring self-diffusion coefficients of protonated systems with a mobile single-sided NMR sensor is discussed. The NMR sensor uses a magnet geometry that generates a highly flat sensitive volume where a strong and highly uniform static magnetic field gradient is defined. Self-diffusion coefficients were measured by Hahn- and stimulated echoes detected in the presence of the uniform magnetic field gradient of the static field. To improve the sensitivity of these experiments, a Carr–Purcell–Meiboom–Gill pulse sequence was applied after the main diffusion-encoding period. By adding the echo train the experimental time was strongly shortened, allowing the measurement of complete diffusion curves in less than 1 min. This method has been tested by measuring the self-diffusion coefficients D of various organic solvents and poly(dimethylsiloxane) samples with different molar masses. Diffusion coefficients were also measured for *n*-hexane absorbed at saturation in natural rubber with different cross-link densities. The results show a dependence on the concentration that is in good agreement with the theoretical prediction. Moreover, the stimulated-echo sequence was successfully used to measure the diffusion coefficient as a function of the evolution time in systems with restricted diffusion. This type of experiment proves the pore geometry and gives access to the surface-to-volume ratio. It was applied to measure the diffusion of water in sandstones and sheep Achilles tendon. Thanks to the strong static gradient G_0, all diffusion coefficients could be measured without having to account for relaxation during the pulse sequence.

Keywords: NMR; Self-diffusion; Static gradient; Unilateral NMR; Cross-linked elastomers; Porous media; Achilles tendon; Restricted diffusion

1. Introduction

In the last years, several applications of NMR in strongly inhomogeneous magnetic fields have been developed. Large field gradients are desired in experiments like STRAFI to image hard materials with high spatial resolution [1], but they are pointed out as disadvantageous in single-sided NMR, where off-resonance effects across the sample complicate the performance of conventional pulse sequences, and reduce the sensitivity during the detection [2,3]. Consequently, the use of open NMR sensors for non-destructive sample characterization required reexamination of conventional pulse sequences to measure relaxation times [4–6], multiple quantum coherences [7,8], images [9,10], and mass transport [11,12], eliminating distortions due to the presence of unavoidable field inhomogeneities. This type of sensor has been successfully applied in material testing [13,14], biomedicine [15], and well logging [16]. Moreover, the first steps toward high-resolution NMR spectroscopy in inhomogeneous fields have been taken and the first ex situ spectra have recently been measured [17–20].

Although in the cases mentioned above, the presence of the static gradient represents a complication to extract the desired information, some applications like high-resolution sample profiling or measurements of diffusion coefficients benefit from it. The biggest difficulty that is faced with an open magnet is the generation of a uniform gradient. Recently, we have presented a simple magnet geometry

* Corresponding author. Fax: +49 241 80 22 185.
E-mail address: bluemich@mc.rwth-aachen.de (B. Blümich).

1090-7807/$ - see front matter © 2006 Elsevier Inc. All rights reserved.
doi:10.1016/j.jmr.2006.02.015

that produces a strong and highly uniform gradient at a defined distance from the magnet surface [21]. It has been used to measure sample profiles with a spatial resolution better than 5 μm, a technique that has opened important new applications to NMR that range from in vivo skin measurements to the characterization of objects of cultural heritage [21,22]. In this paper, we exploit the strong and uniform static gradient of this magnet to measure self-diffusion in a variety of materials to reveal the sample microstructure.

In many systems molecular self-diffusion provides important information on molecular organization and interactions of mobile molecules with the environment. The effect of molecular self-diffusion on the amplitudes of the Hahn and the stimulated echoes in a strong static magnetic-field gradient has been analyzed theoretically and experimentally in recent years [23–29]. The use of strong static gradients such as the one found in the stray field of superconducting magnets, allows measurements of root-mean square molecular displacements as small as 20 nm and self-diffusion coefficients as small as 10^{-16} m^2/s. Large gradients simplify measurements of the diffusion coefficient in heterogeneous materials like porous materials and biological systems, since it reduces the relative contribution from background gradients due to susceptibility variation across the sample. This is so because the background gradients are proportional to the magnitude of the applied static field B_0 but essentially independent of the field gradient. From this point of view, measurements with unilateral low field NMR sensors, which produce relatively strong field gradients, offer an interesting advantage over conventional methods.

Although the possibility of using the strong gradient of an open magnet to measure diffusion has been mentioned in the very first papers about inside-out NMR [2], the need of a uniform gradient complicated the use of hand-held unilateral NMR sensors for accurate determination of diffusion coefficients. The problem was recently alleviated with the implementation of a numerical procedure that deconvolutes the spatial variation of the static field gradient [30]. However, the method requires knowledge of the spatial distribution of both, the B_0 and B_1 fields, and the assumption of a uniform diffusion coefficient D across the sample. It was applied to measurements done with a bar magnet NMR-MOUSE®, where D was extracted for a series of liquids with different viscosities. The effect of relaxation in these self-diffusion measurements was overcome by means of a constant-relaxation method [23,25,30]. The simple pulse sequence $\theta_x - \tau_1 - 2\theta_y - \tau_1 + \tau_2 - 2\theta_y - \tau_2 - \textit{Hahn echo}$ was used to determine the self-diffusion coefficient D at constant-relaxation condition, i.e., for $\tau_1 + \tau_2 = \text{const}$ in the presence of strongly inhomogeneous static and radio-frequency magnetic fields [30]. The method was shown to be particularly useful for measuring D of solvents in elastomers without the need to measure the transverse relaxation rates. Although this numerical procedure provides an alternative to measure diffusion even in the presence of non-uniform gradients, it suffers from limited accuracy compared to conventional techniques like STRAFI. The most important drawback is the need of the B_0 map to extract the distribution of static gradient, a calculation that is an important source of errors.

In this paper, we take advantage of a simple magnet geometry that generates a highly uniform and strong gradient [21] to measure the self-diffusion coefficient of protonated molecules with high accuracy and in very short experimental times. The effect of self-diffusion was encoded in the amplitudes of the stimulated and Hahn echoes generated in the presence of the static magnetic field gradient. The sensitivity of these experiments was improved by applying a Carr–Purcell–Meiboom–Gill (CPMG) pulse sequence after the diffusion-encoding period. Both sequences have been tested by measuring D of various organic solvents, and poly(dimethylsiloxane) (PDMS) samples with different molar masses. The Hahn-echo sequence was used to measure D for n-hexane absorbed at saturation in a natural rubber samples with different cross-link densities. Moreover, the stimulated-echo sequence was used to measure the dependence of the diffusivity on the diffusion time in a water-saturated sandstone as well as in Achilles sheep tendon.

2. Experimental

2.1. Single-sided NMR sensor

The unilateral NMR sensor, used in this work takes advantages of a magnet specially designed to generate a magnetic field with a uniform gradient in the sensitive volume [21]. The geometrical configuration of the permanent magnet is shown in Fig. 1 [21]. It consists of four permanent magnet blocks positioned on an iron yoke. The direction of polarization of each magnet block is indicated by the shades of gray. Magnets with the same polarization are separated by a small gap d_S while magnets with oppo-

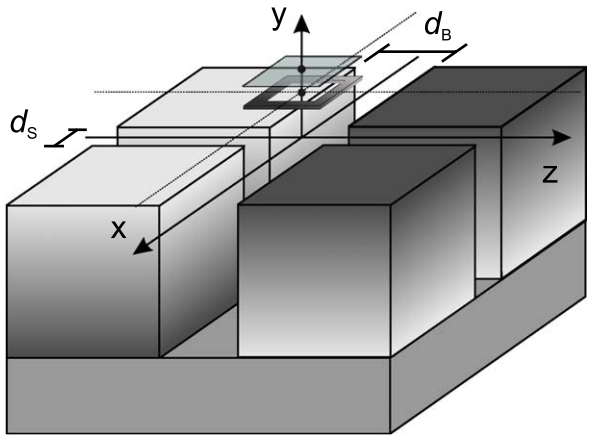

Fig. 1. The magnet geometry used for the one-sided NMR sensor with improved magnetic field gradient uniformity [21]. It consists of four permanent magnet blocks positioned on an iron yoke. The direction of polarization of the magnets is indicated by the gray shades.

site polarization are separated by a larger gap d_B. The distance from the magnet surface where the uniform magnetic field gradient is determined, can be selected by varying d_S and d_B. To find the right gap dimensions which define a constant field along both dimensions at the same depth, one of the two gaps, usually d_B, is set to define the maximum penetration into the sample and the value of d_S is varied to the minimize the field variation at this depth. For a fine tuning of d_S the magnetic field was scanned via NMR resonance [21]. The distance from the magnet surface where the flat slice is generated increases with d_B. At the same time, the field and gradient strength generated in the flat sensitive volume decrease with increasing d_B. Depending on the application, sensors with different gradient strengths can be built. For $d_S = 2$ mm and $d_B = 14$ mm, the flat sensitive slice is defined at 10 mm from the magnet surface. The magnetic field points along the z direction and has a magnitude of about 0.42 T (^{1}H 18.1 MHz), while the magnetic field gradient is 22.36 T/m and points along y direction. The value of the field gradient was determined with high accuracy via self-diffusion experiments of liquids with known diffusion coefficients. More details about the NMR sensor are given in [21].

2.2. Self-diffusion measurements

The pulse sequences used in our investigation are based on Hahn (SGSE)- and stimulated echoes (SGSTE) both operating in the presence of a steady gradient. To improve the sensitivity of these experiments, a CPMG sequence was applied after the main diffusion-encoding period to generate an echo train that takes advantage of long transverse relaxation times of liquid samples (Fig. 2). Thanks to the sensitivity improvement obtained by adding the echo train, a time shorter than one minute was required to measure a complete diffusion curve.

The normalized signal attenuation for the SGSE and the SGSTE are given by [27,28]

$$\ln\left(\frac{I}{I_0}\right) = -\frac{2}{3}\gamma^2 G^2\tau^3 D - \frac{2\tau}{T_2} \tag{1}$$

and

$$\ln\left(\frac{I}{I_0}\right) = -\gamma^2 G^2\tau_1^2\left(\tau_2 + \frac{2}{3}\tau_1\right)D - \frac{2\tau_1}{T_2}, \tag{2}$$

respectively. The time parameters τ_1, τ_2, and τ are defined in Fig. 2, and T_2 is the transverse relaxation time. The ratio gyromagnetic is denoted by γ. The normalization signal I_0 corresponds to the amplitude of the echoes at very small times, τ and τ_2 for SGSE and SGSTE, respectively. The amplitudes of the Hahn and stimulated echoes are attenuated by the transverse and longitudinal relaxation times (see Eqs. (1) and (2)). For large values of D like in the case of less viscous liquids and for strong magnetic field gradients, the diffusion terms in Eqs. (1) and (2) dominate the relaxation terms. Furthermore, if τ, $\tau_1 \ll T_2$, Eqs. (1) and (2) can be approximated by

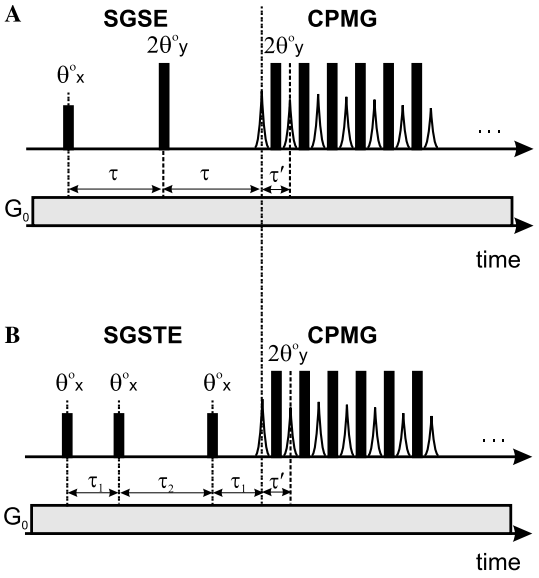

Fig. 2. Constant gradient stimulated echo SGSTE (A) and Hahn echo SGSE (B) pulse sequences used to measure D with the one-sided NMR sensor. The signal-to-noise ratio is improved in both sequences by applying a CPMG train after the diffusion encoding periods.

$$\ln\left(\frac{I}{I_0}\right) \approx -\frac{2}{3}\gamma^2 G^2\tau^3 D \tag{3}$$

and

$$\ln\left(\frac{I}{I_0}\right) \approx -\gamma^2 G^2\tau_1^2\left(\tau_2 + \frac{2}{3}\tau_1\right)D, \tag{4}$$

respectively. Our results below prove that the above equations are valid in a good approximation.

The CPMG echo train is also attenuated by the diffusion process due to the presence of the strong field gradient, however, a small inter-echo time alleviates this effect. Furthermore, the diffusion encoding of the CPMG echo train remains constant during the variation of the time parameters τ_1, τ_2, and τ and does not affect the validity of Eqs. (1)–(4).

The diffusion coefficients were measured on protons at a transmitter frequency of 18.1 MHz with the pulse sequences of Fig. 2 using a 90° and 180° pulses of 10 μs duration. The difference between the pulses is given by the transmitter attenuation.

3. Results and discussion

3.1. Self-diffusion coefficients of liquids with different viscosities

The diffusion coefficients of low viscosity liquids like benzene, *n*-hexane, methanol, ethanol, and hexadecane, taken from our laboratory without further purification, and high viscosity poly(dimethylsiloxane) (Aldrich), with molar masses $M_w = 5000$ g/mol and $M_w = 10{,}000$ g/mol (hereafter PDMS 5000 and PDMS 10,000) have been measured in the uniform field gradient of our one-sided NMR

sensor. The D values are compared with data reported in the literature. The diffusivities of all these liquids were measured with the SGSE and SGSTE methods in combination with a CPMG echo train for detection. The experimental data are shown in Figs. 3 and 4. The data could well be fitted with Eqs. (3) and (4). Hence, the effects of relaxation can be neglected for the applicable ranges of used experimental parameters and diffusivities. The values of D obtained from the fits are given in Table 1. The error measure as the variance of a set of similar experiments is of the order of 1%. The D values obtained by the two different methods agree well with each other and the values from literature (see Table 1).

3.2. Proton self-diffusion of n-hexane in natural rubber with different cross-link densities

The diffusion of light penetrant molecules in elastomers is a topic of long standing interest [31] (and references therein). It was shown that for small solvent molecules, both the transverse relaxation time and the diffusion coefficient are sensitive measures of the free volume and its changes with the filler content [32,33]. The basic formulation used by Ventras and Ventras [34] for the prediction of the diffusion coefficient in an isotropic rubbery polymer–solvent system is based on the expression:

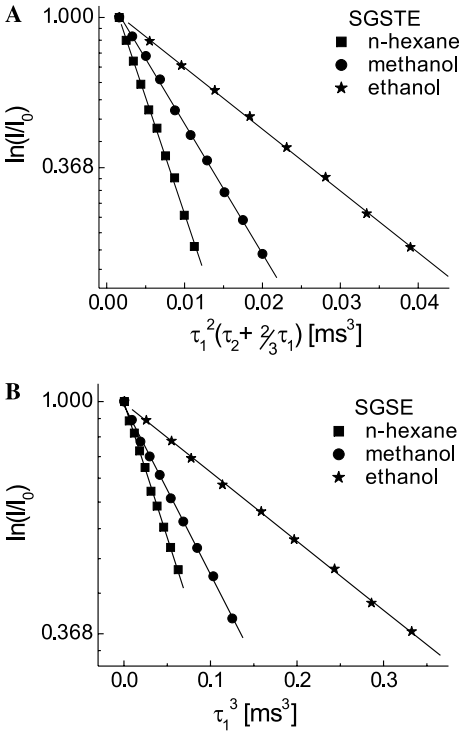

Fig. 3. Diffusion curves of different organic liquids measured with the CGSE/CPMG (A) and CGHE/CPMG (B) pulse sequences (Fig. 2). In all measurements four scans a repetition delay (RD) of 5 s were used. For sensitivity improvement 1024 echoes ($\tau' = 0.04$ ms) generated during the CPMG detection period were co-added. In the SGSTE sequence the diffusion time was $\tau_2 = 1$ ms.

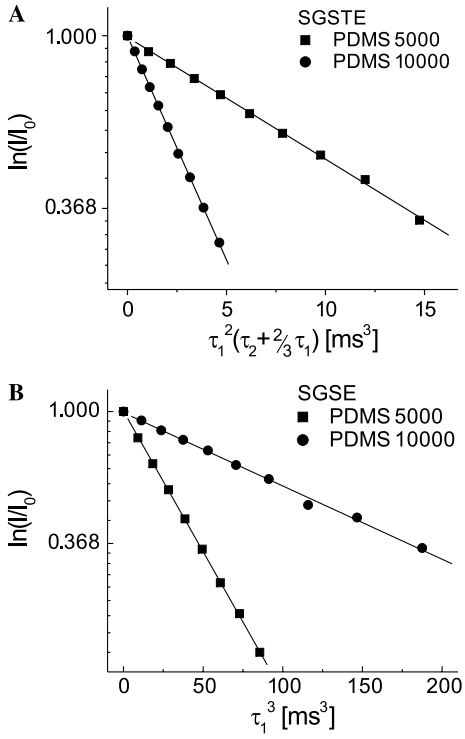

Fig. 4. Diffusion curves of PDMS samples with two molar masses (5000 and 10,000 g/mol) measured with SGSTE/CPMG (A) and SGSE/CPMG (B). In the SGSTE sequence the diffusion time was $\tau_2 = 50$ ms. For sensitivity improvement 1024 echoes ($\tau' = 0.04$ ms) generated during the CPMG detection period were co-added. The total experimental time was about 3 min with 16 scans and RD = 1 s.

Table 1
Self-diffusion coefficients D of various protonated liquids measured by SGSTE and SGSE methods at 22 °C

Sample	D_{lit}[a] [10^{-9} m^2/s]	D_{SGSTE} [10^{-9} m^2/s]	D_{SGSE} [10^{-9} m^2/s]
Benzene	2.11	2.12	2.12
n-Hexane	3.96	4.02	3.90
Methanol	2.271	2.20	2.20
Ethanol	1.01	1.00	1.01
Hexadecane		0.35	0.35
PDMS 5000		7.23×10^{-2}	7.13×10^{-2}
PDMS 10,000		1.97×10^{-2}	1.87×10^{-2}

Literature values reported at 25 °C were corrected using the temperature dependence of viscosity and Stokes equation.
[a] Corrected from the values reported in the Bruker Almanac 2005.

$$\ln D = \ln \overline{D}_0 - \frac{E^*}{RT} - \left\{ \frac{w_s \hat{V}_1^* + \xi(1-w_s)\hat{V}_2^*}{\hat{V}_{FH}/\gamma} \right\}, \tag{5}$$

where D is the diffusion coefficient of the penetrant. $\overline{D}_0$ is an effectively constant pre-exponential factor, E^* is the effective energy/mol that a molecule needs to overcome attractive forces, R is the universal gas constant, T is the absolute temperature, and w_s is the sorbed solvent weight fraction. The specific free volume required for a jump of penetrant and polymer are denoted by $\hat{V}_1^*$ and $\hat{V}_2^*$, respectively. The significance of the other quantities is given in [34].

The results of sorption experiments are expressed in general as moles Q_w of liquid sorbed by 100 g of NR. The quantity Q_w measured in mole % is determined as

$$Q_w = \frac{(\text{Weight of sorbed solvent})/(\text{Molecular weight of the solvent})}{\text{Initial weight of rubber}} \times 100\%. \quad (6)$$

From Eqs. (5) and (6) we can get

$$\ln D = \ln \overline{D}_0 - \frac{E^*}{RT} - \frac{\xi \hat{V}_2^*}{\hat{V}_{FH}/\gamma} - \frac{\hat{V}_1^* - \xi \hat{V}_2^*}{\hat{V}_{FH}/\gamma} \frac{Q_w M_{w,s}}{Q_w M_{w,s} + 1}, \quad (7)$$

where $M_{w,s}$ is the molecular weight of the solvent.

In this work we measured the diffusion coefficients of *n*-hexane swollen in a series of cross-linked natural rubber (NR) SMR10 (Malaysia) (cf. Table 1) by the diffusion encoding of the Hahn echo amplitude in the stray field of the sensor. The additives were 3 phr (parts-per-hundred-rubber) ZnO and 2 phr stearic acid. The sulfur and accelerator contents of the samples are given in Table 2. The accelerator is of the standard sulfenamide type (TBBS, benzothiazyl-2-*tert*-butyl-sulfenamide). After mixing the compounds in a laboratory mixer at 50 °C, the samples were vulcanized at 160 °C in a Monsanto MDR-2000-E vulcameter. The degree of cross-linking was measured by the low frequency shear modulus or torque at a temperature of 160 °C in the vulcameter directly after vulcanisation. The measurements were performed with an oscillation amplitude of ±0.5° and a frequency of 1.67 Hz.

The natural rubber samples were swollen in *n*-hexane for several hours until the equilibrium value was reached. Besides the direct mixing, swelling in *n*-hexane vapours was also tested. In the limit of experimental errors the diffusivities do not change as a function of the swelling protocol. The decay of the Hahn echo for *n*-hexane sorbed in NR was fitted by a sum of an exponential function that depends on τ^3 and an exponential decay linear on τ that describe the T_2 signal decay of the polymer network itself (Fig. 5A). The logarithm of the diffusion coefficient versus the solvent mole percent concentration at equilibrium for a series of cross-linked NR samples is shown in Fig. 5B. In a good approximation the experimental data follow the functional dependence on Q_w given by Eq. (7).

Table 2
Properties of the series of cross-linked NR samples

Sample	Sulfur–accelerator content (phr)	Shear modulus[a] G (dNm)	Equilibrium toluene concentration[b] c_s (%)
NR1	1–1	5.2	0.652
NR2	2–2	8.5	0.671
NR3	3–3	11.2	0.678
NR4	4–4	13.2	0.692
NR5	5–5	14.5	0.712
NR6	6–6	15.4	0.750
NR7	7–7	16.2	0.800

[a] The uncertainties are less than 10%.
[b] The uncertainties are less than 1%.

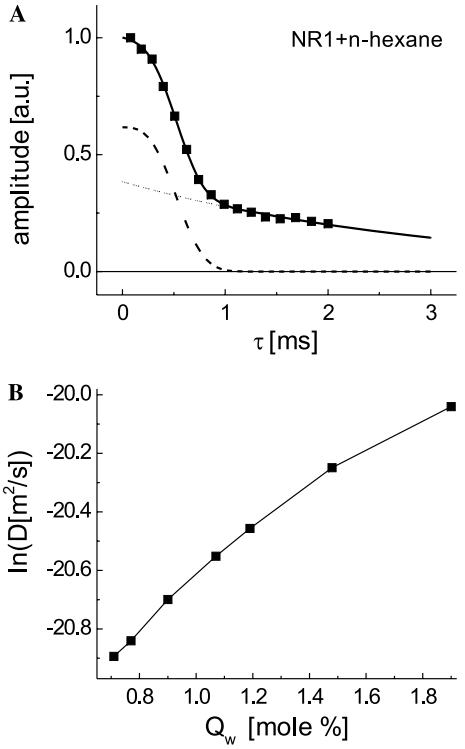

Fig. 5. (A) Amplitude of the NMR signal of SGSE/CPMG pulse sequence as a function of τ for *n*-hexane sorbed in NR1 sample (Table 2). The protons from the solvent as well as the ones from natural rubber contribute to the Hahn-echo amplitude (squares). The data can be fitted (solid line) by the addition of an exponential decay in τ^3 (dashed line) and a single exponential decay (thin-dashed line) in τ. The diffusivity of *n*-hexane can be determined from the exponential decay in τ^3 (Eq. (3)). The total experimental time was of about 6 min. (B) Natural logarithm of the diffusion coefficients as a function of the *n*-hexane mole concentration Q_W for the natural rubber series of Table 2. The quantity Q_w is defined as the number of moles of *n*-hexane absorbed in 100 g of natural rubber. The data points are connected by lines and show a trend according to Eq. (7).

3.3. Self-diffusion of water in saturated sandstone

The measurements of the diffusion of liquids adsorbed in the pores of catalysts and rocks are strongly affected by the presence of barriers [27,28]. It can be used to establish the average pore sizes, pore size distributions, and tortuosity [35,36].

The time-dependent diffusion coefficient D of water was measured by the CGSE method discussed above (see Section 2.2) for two sandstone cores obtained from the Integrated Ocean Drilling Program (IODP) (Sandstone A and B in Fig. 6). Standard IODP geological cores have a diameter of about 60 mm and a length of 1.5 m. Right after drilling they are split into half-cylinders along the core axis. The decays of the stimulated echoes from water-saturated IODP cores follow Eq. (4) and were fitted in a semi-log plot by a linear function. The time-dependent D coefficients are shown in Fig. 6 as a function of the diffusion length L_D (see below).

For short diffusion times τ_2, the diffusion coefficient $D(\tau_2)$ is expected to fall off linearly with the diffusion length

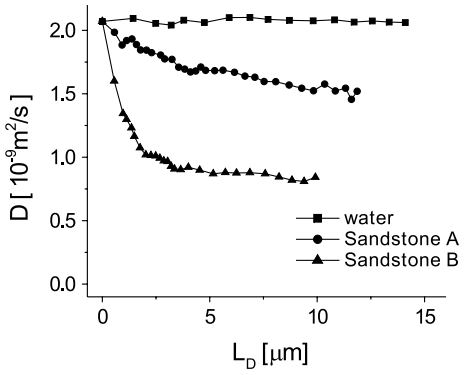

Fig. 6. Time-dependent diffusion coefficient D of bulk water, and two different sandstone cores (A and B) measured by the SGSTE/CPMG method as a function of the diffusion length $L_D = \sqrt{D_0\tau_2}$. The bullet symbol marks the diffusion coefficient of free water $D_0 = 2.07 \times 10^{-9}$ m^2/s to which $D(L_D)$ should extrapolate in the limit of $L_D \to 0$. The total experimental time is about 20 min per point with 256 scans and RD = 0.5 s.

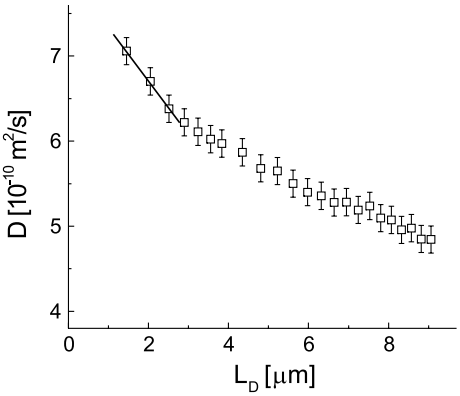

Fig. 7. Time-dependent diffusion coefficient D of water in sheep Achilles tendon measured by the SGSTE/CPMG method as a function of the diffusion length $L_D = \sqrt{D_0\tau_2}$. The solid line shows the fit of the experimental data with Eq. (8). The total experimental time is about 20 min per point with 256 scans and RD = 0.5 s.

[35], with a slope proportional to the medium surface-to-volume ratio (S/V), i.e.

$$D(L_D) \approx D_0\left[1 - \frac{4}{9\sqrt{\pi}}\frac{L_D S}{V}\right]. \quad (8)$$

The diffusion length L_D in Eq. (8) is defined as $L_D = \sqrt{D_0\tau_2}$, where $D_0 = \lim_{\tau_2 \to 0} D(\tau^2)$. The diffusion length was calculated approximating D_0 by the value by of the diffusion coefficient of free water. By taking this approximation from the linear fit of the data in Fig. 6, the average volume-to-surface ratio V/S for the pores in the sandstone cores was determined to be of the order of 5 and 0.6 μm for sample A and B, respectively. In the approximation of spherical pores we can estimate an average pore radius of $\bar{r}_A \approx 15$ μm and $\bar{r}_B \approx 2$ μm. Nevertheless, for sample B the quantity V/S cannot be measured accurately because the stimulated echo method does not give access to short enough diffusion lengths L_D. The reason for this has been discussed in [36] and is related to the failure of the narrow pulse approximation for short diffusion times.

3.4. Self-diffusion of water in sheep Achilles tendon

The time-dependent diffusion coefficient of water in Achilles tendons is anisotropic, diffusion-time dependent, and changes as a function of tensile load [37,38]. The diffusion measurements reveal two diffusion process characterized by a fast and a slow diffusion process [38].

Samples of sheep Achilles tendon were obtained from the butcher. The samples were kept at −18 °C after excision until the time of measurement and then measured at room temperature 20 °C ± 1 °C. A plug was cut from the middle of the tendon and wrapped with parafilm in order to avoid dehydration. The plug was examined for about 12 h at room temperature and then discarded to preclude tissue degradation. The sample was prepared by cutting a piece of the tendon along the symmetry axis of the tissue.

Our measurements based on the CGST/CPMG method report only the diffusion coefficient of the fast process valid in the regime of small τ_1. In all the measurements the plug axis was oriented along the direction of the static magnetic field. From the linear fit of the initial diffusivity data in Fig. 7, the average volume-to-surface ratio V/S for the pores in sheep Achilles tendon was determined to be $V/S \approx 8$μm assuming D_0 to be the value of the free water.

4. Conclusions

In this work we demonstrate that implementing Hahn and stimulated-echo sequences on a mobile NMR sensor with a uniform static gradient, self-diffusion coefficients down to 10^{-12} m^2/s can be measured. Such small diffusion coefficients can be acceded because of the strong field gradient of the magnetic field ($G \sim 20$ T/m). The NMR sensor has a special magnet geometry that generates a strong and uniform field gradient in a flat sensitive volume of about 1×1 cm^2 extended along the lateral directions positioned at a defined distance from the magnet surface. The measurement time was reduced to minutes by the use of a CPMG echo train applied after the encoding sequence.

The mobile NMR sensor with a well-defined magnetic field gradient was used to measure the diffusion coefficients of solvents swollen in cross-linked elastomers. The experiments were performed on a series of samples of natural rubber and have shown that the diffusion coefficients correlate with the cross-link density. This technique constitutes an alternative to measuring the transverse magnetization relaxation for information about the cross-link density of elastomers. Moreover, this method shows potential applications for characterizing polymer networks like defect distributions, and for testing the theory of polymer swelling. Moreover, this mobile NMR sensor can be used for characterization of pore surface-to-volume ratios and pore sizes in rocks and ordered tissues.

The possibility to perform diffusion measurements in combination with a CPMG pulse sequence with our specially designed one-sided NMR mobile sensor can also be exploited for measurements of two-dimensional D-T_2 maps [39]. Therefore, the device can be used for quality controls of complex materials.

References

[1] P.J. McDonald, Stray field magnetic resonance imaging, Prog. Nucl. Magn. Reson. Spect. 30 (1997) 69–99, and references therein.

[2] R.L. Klinberg, A. Sezginer, D.D. Griffin, M. Fukuhara, Novel NMR apparatus for investigating an external sample, J. Magn. Reson. 97 (1992) 466–485.

[3] G. Eidmann, R. Savelsberg, P. Blümler, B. Blümich, The NMR MOUSE, a mobile universal surface explorer, J. Magn. Reson. A 122 (1992) 104–109.

[4] G. Goelman, M.G. Prammer, The CPMG pulse sequence in strong magnetic field gradients with applications to oil-well logging, J. Magn. Reson. A 113 (1995) 11–18.

[5] M.D. Hürlimann, D.D. Griffin, Spin dynamics of Carr–Purcell–Meiboom–Gill-like sequences in grossly inhomogeneous B_0 and B_1 fields and application to NMR well logging, J. Magn. Reson. 143 (2000) 120–135.

[6] F. Balibanu, K. Hailu, K. Eymael, D.E. Demco, B. Blümich, Nuclear magnetic resonance in inhomogeneous magnetic fields, J. Magn. Reson. 145 (2000) 246–258.

[7] A. Wiesmath, C. Filip, D.E. Demco, B. Blümich, Double-quantum filtered NMR signals in inhomogeneous magnetic fields, J. Magn. Reson. 149 (2001) 258–263.

[8] A. Wiesmath, D.E. Demco, B. Blümich, NMR of multipolar spin states excited in strongly inhomogeneous magnetic fields, J. Magn. Reson. 154 (2002) 60–72.

[9] F. Casanova, J. Perlo, B. Blümich, K. Kremer, Multi-echo imaging in highly inhomogeneous magnetic fields, J. Magn. Reson. 166 (2004) 76–81.

[10] J. Perlo, F. Casanova, B. Blümich, 3D imaging with a single-sided sensor: an open tomograph, J. Magn. Reson. 166 (2004) 228–235.

[11] F. Casanova, J. Perlo, B. Blümich, Velocity distributions remotely measured with a single-sided, J. Magn. Reson. 171 (2004) 124–130.

[12] J. Perlo, F. Casanova, B. Blümich, Velocity imaging by ex situ NMR, J. Magn. Reson. 173 (2005) 254–258.

[13] A. Guthausen, G. Zimmer, P. Blümler, B. Blümich, Analysis of polymer materials by surface NMR via the NMR MOUSE, J. Magn. Reson. 130 (1998) 1–7.

[14] K. Hailu, R. Fechete, D.E. Demco, B. Blümich, Segmental anisotropy in strained elastomers detected with a portable NMR scanner, Solid State Nucl. Magn. Reson. 22 (2002) 327–343.

[15] R. Haken, B. Blümich, Anisotropy in tendon investigated in vivo by a portable NMR scanner, J. Magn. Reson. 144 (2000) 195–199.

[16] R.L. Klingberg, in: Encyclopedia of Nuclear Magnetic Resonance, vol. 8, chapter Well logging, Wiley, 1996, pp. 4960–4969.

[17] C.A. Meriles, D. Sakellariou, H. Heise, A.J. Moulé, A. Pines, Approach to high-resolution ex situ NMR spectroscopy, Science 293 (2001) 82–85.

[18] H. Heise, D. Sakellariou, C.A. Meriles, A.J. Moulé, A. Pines, Two-dimensional high-resolution NMR spectra in matched B_0 and B_1 field gradients, J. Magn. Reson. 156 (2001) 146–151.

[19] C. Meriles, D. Sakellariou, A. Pines, Resolved magic-angle spinning of anisotropic samples in inhomogeneous fields, Chem. Phys. Lett. 358 (2002) 391–395.

[20] J. Perlo, V. Demas, F. Casanova, C.A. Meriles, J. Reimer, A. Pines, B. Blümich, High-resolution NMR spectroscopy with a portable single-sided sensor, Science 308 (2005) 1278–1279.

[21] J. Perlo, F. Casanova, B. Blümich, Profiles with microscopic resolution by single-sided NMR, J. Magn. Reson. 176 (2005) 64–70.

[22] F. Casanova, J. Perlo, B. Blümich, Depth profiling by single-sided NMR, in: S. Stapf, S. Han (Eds.), Nuclear Magnetic Resonance Imaging in Chemical Engineering, Wiley-VCH, Weinheim, 2005.

[23] R. Kimmich, W. Unrath, G. Schnur, E. Rommel, NMR measurements of small diffusion experiments in the fringe field of superconducting magnets, J. Magn. Reson. 91 (1991) 136–140.

[24] G. Fleischer, F. Fujara, Segmental diffusion in polymer melts and solutions of poly(ethylene oxide) measured with field gradient NMR in high-field gradients, Macromolecules 25 (1992) 4210–4219.

[25] D.E. Demco, A. Johansson, J. Tegenfeldt, Constant-relaxation methods for diffusion measurements in the fringe field of superconducting magnets, J. Magn. Reson. A 110 (1994) 183–193.

[26] A. Scharfenecker, I. Ardelean, R. Kimmich, Diffusion measurements with the aid of nutation spin echoes appearing after two inhomogeneous radiofrequency pulses in inhomogeneous magnetic fields, J. Magn. Reson. 148 (2001) 363–366.

[27] P.T. Callaghan, Principles of Magnetic Resonance Microscopy, Clarendon Press, Oxford, 1991.

[28] R. Kimmich, NMR: Tomography, Diffusiometry, Relaxometry, Springer-Verlag, Berlin, Heidelberg, New York, 1997.

[29] M.D. Hürlimann, Diffusion and relaxation effects in general stray field NMR experiments, J. Magn. Reson. 148 (2001) 367–378.

[30] M. Klein, R. Fechete, D.E. Demco, B. Blümich, Self-diffusion measurements by a constant-relaxation method in strongly inhomogeneous magnetic fields, J. Magn. Reson. 164 (2003) 310–320.

[31] E.D. van Meerwall, Self-diffusion in polymer systems measured with field-gradient spin echo NMR methods, Adv. Polym. Sci. 54 (1983) 1–29.

[32] E.D. van Meerwall, D. Shook, Self-diffusion of C_6F_6 in filled rubbery polymers, J. Appl. Phys. 56 (1984) 2444–2447.

[33] D.E. Demco, G. Rata, R. Fechete, B. Blümich, Self-diffusion anisotropy of small penetrant molecules in deformed elastomers, Macromolecules 38 (2005) 5647–5653.

[34] J.S. Ventras, C.M. Ventras, Solvent self-diffusion in rubbery polymer–solvent system, Macromolecules 27 (1994) 4684–4690 (and references therein).

[35] P.P. Mitra, P.N. Sen, L.M. Schwartz, Short-time behaviour of diffusion coefficients as a geometrical probe of porous media, Phys. Rev. B 47 (1993) 8565–8575.

[36] L.J. Zielinski, M.D. Hürlimann, Probing short length scales with restricted diffusion in a static gradient using the CPMG sequence, J. Magn. Reson. 172 (2004) 162–168.

[37] J. Wellen, K.G. Helmer, P. Grigg, C.H. Sotak, Application of porous-media theory to the investigation of water ADC changes in rabbit Achilles tendon caused by tensile loading, J. Magn. Reson. 170 (2004) 49–55.

[38] R. Fechete, D.E. Demco, U. Eliav, B. Blümich, G. Navon, NMR Biomed. 18 (2005) 577–586.

[39] M.D. Hürlimann, L. Venkataramanan, Quantitative measurement of two-dimensional distribution functions of diffusion and relaxation in grossly inhomogeneous fields, J. Magn. Reson. 157 (2002) 31–42.